Electronic Supplementary Material (ESI) for Chemical Science.

Supporting Information

Quinoline-Containing Diarylethenes: Bridging Between Turn-On Fluorescence, RGB Switching and Room Temperature Phosphorescence

Zhen Xu, Qian T. Liu, Xiaozhu Wang, Qian Liu, Duane Hean, Keng C. Chou and Michael O. Wolf*

General

^{1}H and $^{13}P\{^{1}H\}$ NMR spectroscopic data were collected on a 400 MHz Bruker Avance 400 spectrometer at 25 °C. Chemical shifts are referenced to the residual solvent signals. X-ray crystallography data were collected on a Bruker X8 APEX II diffractometer with graphite monochromated Mo-Kα radiation. ESI mass spectra were collected using a Waters LC-MS ESI mass spectrometer. Absorption spectra were obtained on a Varian Cary 5000 UV-Vis-NIR spectrophotometer. Steady-state fluorescence data were collected on a Photon Technology International (PTI) QuantaMaster 50 fluorimeter fitted with an integrating sphere, double excitation monochromator and utilizing a 75 W Xe arc lamp as the source. Emission decays were measured on a Horiba Jobin Yvon Fluorocube equipped with a 359 nm Horiba spectral LED and time-resolved spectra were measured using a Photon Technology International (PTI) QuantaMaster 400. Low temperature studies were conducted on an Oxford Instruments Optistat DN using an ITC610 temperature controller. All syntheses involving air sensitive compounds were carried out using standard Schlenk-type procedures under an atmosphere of N_2. All purchased chemicals were used without further purification. 3-Iodo-2-methyl benzo[*b*]thiophene was synthesized following the literature procedure.[1]

SMLM Setup

Imaging was performed using a home-built microscope with a sample stabilization system. The details of the microscope has been published previously.[2] A 532 nm laser (Opus, Laser Quantum) was used for activation, excitation and deactivation. The laser was coupled into an inverted microscope equipped with an apochromatic TIRF oil-immersion objective lens (60×; numerical aperture 1.49; Nikon). The fluorescence was separated using appropriate dichroic mirrors and filters (Semrock) and detected by an electron multiplying charge-coupled device camera (iXon Ultra, Andor). A feedback loop was employed to lock the position of the sample during image acquisition. Sample drift was controlled to be < 1 nm laterally and 3 nm axially. Fluorescent beads (F8799, ThermoFisher Scientific) were coated onto a coverslip as fiducial markers. Custom software written in MATLAB (Mathworks) was used to reconstruct SMLM images.[2]

Cellular Imaging

HeLa cells were purchased from the American Type Culture Collection (ATCC). Cells were grown in Eagle's Minimal Essential Medium (MEM) supplemented with heat-inactivated 10% fetal bovine serum, 1 mM sodium pyruvate, 4 mM L-glutamine, and 1% nonessential amino acids in a humidified incubator at 37 °C and 5% CO_2. Cells were seeded to culture slips 24 h prior to treatment. The **1o** working solution for fluorescence microscopy was prepared from a DMSO stock solution (4 mM). Cells were exposed to 25 uM **1o** for 2 hours before fixing. Imaging was done using a fluorescence microscope BX40, a U-MWU filter cube, an F-View CCD Camera (all Olympus), Cell-F fluorescence imaging software (Olympus) and a 60X magnification oil immersion objective lens. Video was recorded using an IX70 inverted fluorescence microscope Olympus with a DP80 dual CCD 12.7 megapixel colour camera.

Computational Details

Density functional theory (DFT) calculations were carried out using the Gaussian 16 Rev.C01 suite of programs.[3] The PBE0 functional[4-5] with 6-31G(d,p) basis set was employed to optimize the geometry of the ground-states (S0) of compound **3** in both parallel and anti-parallel conformation. No imaginary frequency was found after the optimization.

Synthesis

2-methylbenzo[*b*]thiophene pinacol boronic ester. 3-Iodo-2-methyl benzo[*b*]thiophene (1.920 g, 7.00 mmol, 1.0 equiv.), bis(pinacolato)diboron (1.950 g, 7.70 mmol, 1.1 equiv.), potassium acetate (2.000 g, 21.00 mmol, 3.0 equiv.) and [1,1'-bis(diphenylphosphino)ferrocene]dichloropalladium(II) (0.171 g, 0.21 mmol, 0.03 equiv.) were added to a Schlenk flask under N_2. Degassed dimethyl sulfoxide (25 mL) was then added. The mixture was stirred at 80 ^oC overnight under a nitrogen atmosphere. The reaction mixture was poured into H_2O (25 mL) and extracted with CH_2Cl_2 (3 × 25 mL). The organic layers were combined and dried over anhydrous $MgSO_4$, filtered and concentrated *in vacuo*. The crude mixture was purified by column chromatography (silica, 30:1 hexanes : EtOAc), yielding the pure compound as a white solid. (1.343 g, 70%). ^1H and $^{13}C\{^1H\}$ NMR data are consistent with literature.[1]

3,4-bis(2-methylbenzo[b]thiophen-3-yl)isoquinoline (1o). 3,4-Dibromoisoquinoline (0.287 g, 1.00 mmol, 1.0 equiv.), 2-methylbenzo[*b*]thiophene pinacol boronic ester (0.600 g, 2.20 mmol, 2.2 equiv.), potassium carbonate (0.545 g, 4.00 mmol, 4.0 equiv.) and tetrakis(triphenylphosphine)palladium(0) (0.116 g, 0.10 mmol, 0.1 equiv.) were added to a Schlenk flask under N_2. Degassed 1,6-dioxane (8 mL) and deionized water (2 mL) were then added. The mixture was stirred at 90 ^oC for 48 hours under a

nitrogen atmosphere. The reaction mixture was poured into H_2O (25 mL) and extracted with CH_2Cl_2 (3× 25 mL). The organic layers were combined and dried over anhydrous $MgSO_4$, filtered and concentrated *in vacuo*. The crude mixture was purified by column chromatography (silica, 2:1 hexanes: EtOAc), yielding the pure compound as a white solid. (0.270 g, 64 %). ^{1}H NMR (400 MHz, CD_2Cl_2) δ 9.52 (s, 1 H), 8.19 (d, 1 H), 7.77 – 6.87 (m, 11 H), 2.31(s, 1.5 H), 2.22 (s, 1.5 H), 1.88 (s, 3 H). ^{13}C{^{1}H} NMR (101 MHz, CD_2Cl_2) δ 153.2, 148.7, 148.6, 141.1, 141.0, 140.60, 140.5, 140.1, 139.7, 139.3, 139.3, 138.7, 138.6, 138.54, 138.2, 136.7, 136.67, 133.7, 133.1, 131.3, 131.2, 128.9, 128.6, 128.5, 128.4, 128.3, 128.3, 128.1, 128.1, 127.2, 127.0, 126.3, 126.0, 125.4, 124.4, 124.3, 124.2, 124.1, 124.1, 124.0, 123.9, 123.5, 123.3, 123.3, 123.2, 122.5, 122.2, 122.2, 121.9, 15.8, 15.7, 15.7, 15.4. ESI-HR MS Calcd. for $C_{27}H_{19}NS_2$: 421.0959; Found: 422.1038 $[M+H]^+$

3,3'-(isoquinoline-3,4-diyl)bis(2-methylbenzo[*b*]thiophene 1,1-dioxide) (2o). To a solution of **1o** (0.126 g, 0.30 mmol, 1.0 equiv) in CH_2Cl_2 (10 mL) at 0 °C was added *m*- chloroperoxybenzoic acid (70%, 0.297 g, 1.20 mmol, 4.0 equiv) and the mixture was stirred for 2 hours. The reaction mixture was poured over a saturated aqueous solution of sodium bicarbonate (15 mL) and was then extracted with CH_2Cl_2 (3 × 10 mL). The organic layers were combined, dried over anhydrous $MgSO_4$, filtered, and concentrated in *vacuo*. The crude mixture was purified by column chromatography (silica, 2:3 hexanes:EtOAc) yielding the pure compound as a yellow solid (0.078 g, 54 %). ^{1}H NMR (400 MHz, CD_2Cl_2) δ 9.58 (s, 1 H), 8.28-8.24 (m, 1 H), 7.87 – 7.63 (m, 8.5 H), 7.10 – 7.05 (m, 1.5 H), 6.79 – 6.65 (m, 1 H), 2.00 (s, 4 H), 1.70 (s, 2 H). ^{13}C{^{1}H} NMR (101 MHz, CD_2Cl_2) δ 155.2, 143.8, 143.7, 140.8, 140.6, 139.7, 138.8, 136.5, 136.4, 136.2, 136.0, 134.9, 134.7, 134.7, 134.0, 133.9, 133.5, 133.4, 133.3, 133.0, 132.8, 132.7, 130.5, 130.4, 130.1, 129.9, 129.9, 129.3, 129.1, 128.7, 125.6, 125.1, 124.4, 124.1, 123.5, 123.0, 122.3, 122.0, 122.0, 121.7, 54.5, 54.3, 54.3, 54.0, 53.7, 53.5, 9.3, 9.0, 8.90, 8.6. ESI-HR MS Calcd. for $C_{27}H_{19}NO_2S_2$: 485.5720; Found: 486.0833 $[M+H]^+$

2-methyl-3,4-bis(2-methylbenzo[*b*]thiophen-3-yl)isoquinolin-2-ium tetrafluoroborate (3). To a solution of **1o** (0.042 g, 0.10 mmol, 1.0 equiv) in toluene (2 mL) was added MeI (1 mL) and the mixture was heated to reflux overnight. The reaction mixture was cooled to room temperature and the solvent removed *in vacuo*. The crude product was dissolved in THF and an excess of NH_4BF_4 aqueous solution was added. The resultant mixture was filtered, washed with deionized water and dried under vacuum to yield pure product as a yellow solid (0.044 g, 84 %). ^{1}H NMR (400 MHz, CD_2Cl_2) δ 10.24 (s, 0.5 H), 10.22 (s, 0.5 H), 8.78-8.75 (m, 1 H), 8.12 – 8.11 (m, 2 H), 7.81 – 7.77 (m, 1 H), 7.68 – 7.55 (m, 2 H), 7.39 – 7.19 (m, 4 H), 7.12 – 6.97 (m, 1 H), 6.85-6.81 (m, 1 H), 4.30 (s, 1.5 H), 4.27 (s, 1.5 H), 2.36 (s, 1.5 H),

2.30 (s, 1.5 H), 2.06 (s, 1.5 H), 1.91 (s, 1.5 H). $^{13}C\{^{1}H\}$ NMR (101 MHz, CD_2Cl_2) δ 153.7, 153.5, 145.2, 144.9, 142.1, 141.8, 141.0, 140.9, 140.7, 140.0, 139.0, 138.9, 138.8, 138.7, 138.6, 138.4, 138.2, 136.6, 136.2, 132.6, 132.5, 132.4, 132.3, 128.1, 126.8, 126.6, 125.9, 125.7, 125.6, 125.5, 125.1, 125.1, 124.9, 124.5, 124.3, 123.3, 122.9, 122.8, 122.7, 122.7, 122.3, 122.1, 121.8, 54.5, 54.5, 54.3, 54.2, 54.0, 53.7, 53.5, 47.9, 16.2, 16.1, 16.0, 15.9. ESI-HR MS Calcd. for $C_{28}H_{22}BF_4NS_2$: 523.4141; Found: 436.1193 $[M\text{-}BF_4]^+$

Photophysical Data

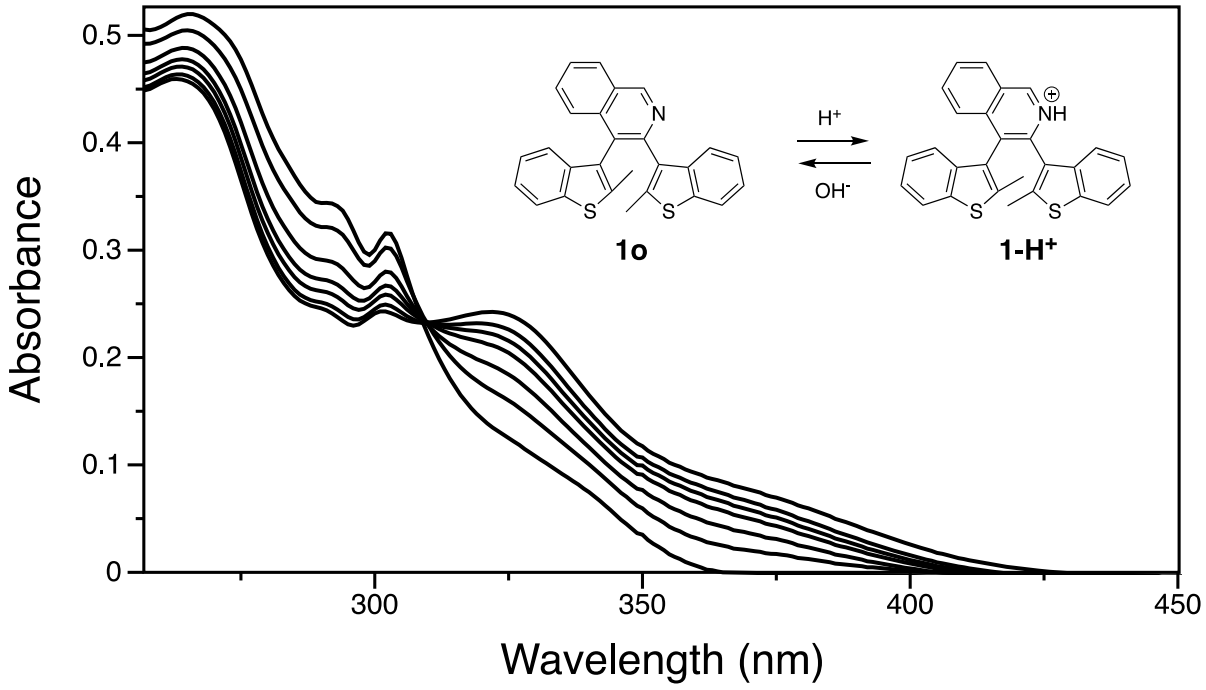

Figure S1. Absorption spectral changes of **1o** (2.5×10^{-5} M) in dichloromethane (DCM) with TFA added.

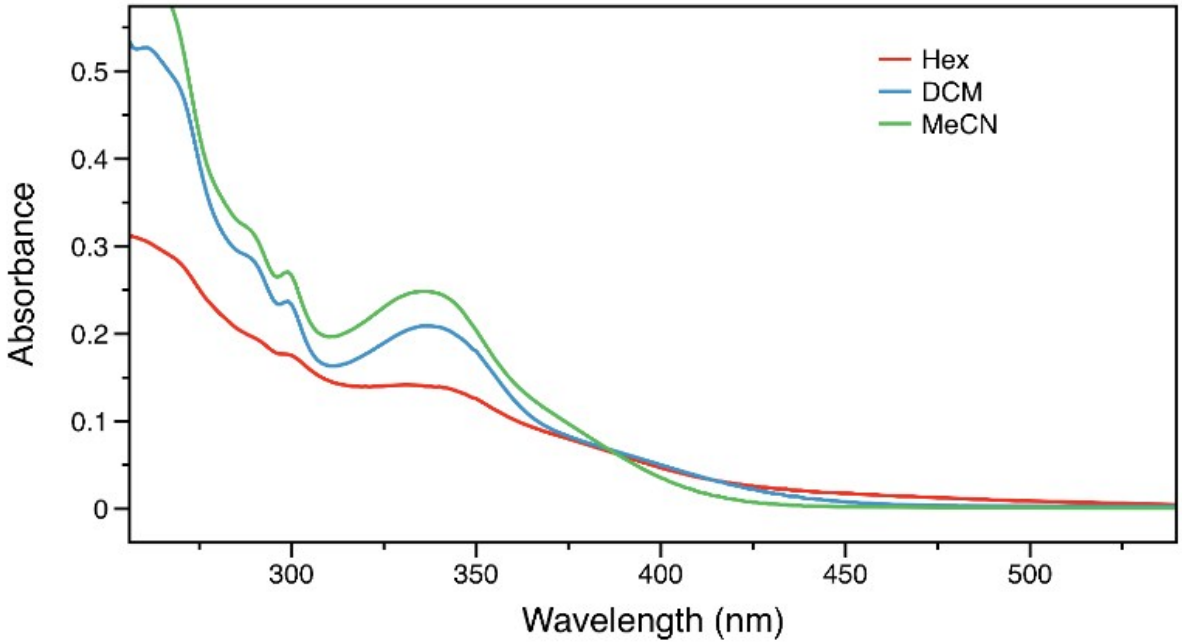

Figure S2. Absorption spectra of **3** (2.5×10^{-5} M) in hexanes (Hex), dichloromethane (DCM) and acetonitrile (MeCN).

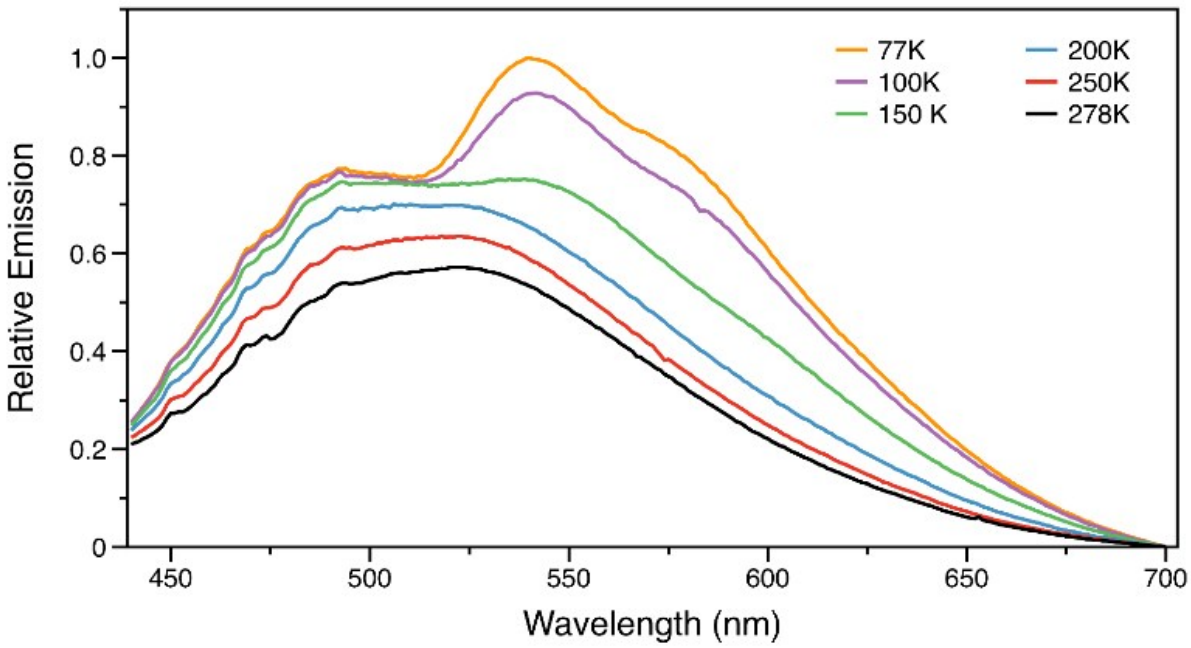

Figure S3. Variable-temperature fluorescence spectra of **3** in the solid state. (λ_{ex} = 380 nm).

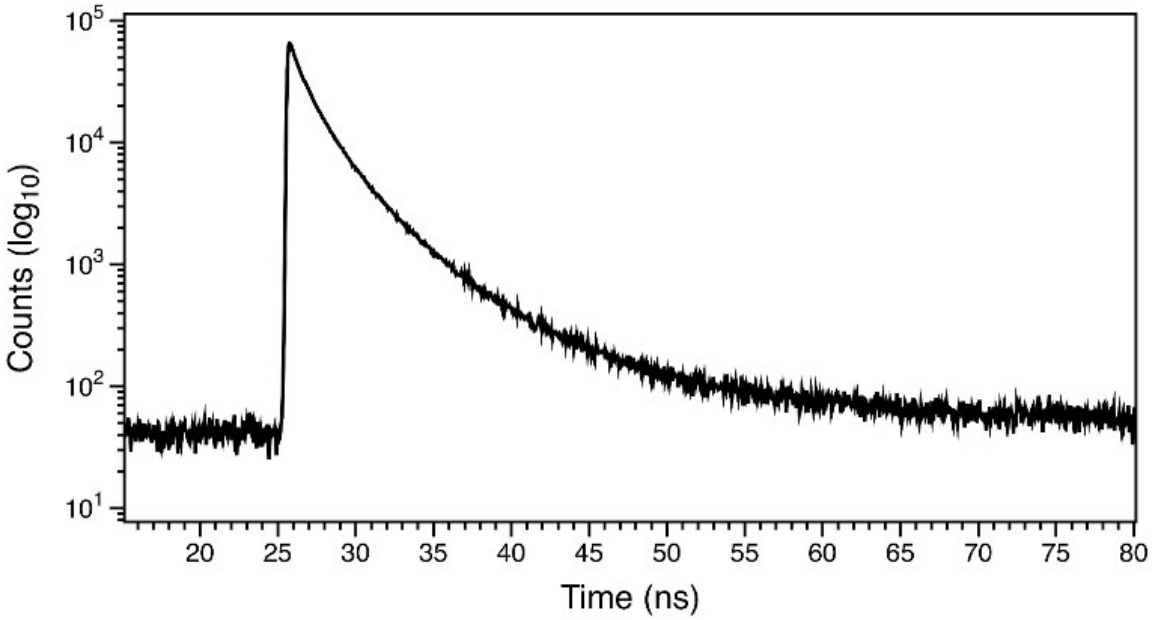

Figure S4. PL lifetime of **3** in the solid state. (λ_{ex} = 359 nm).

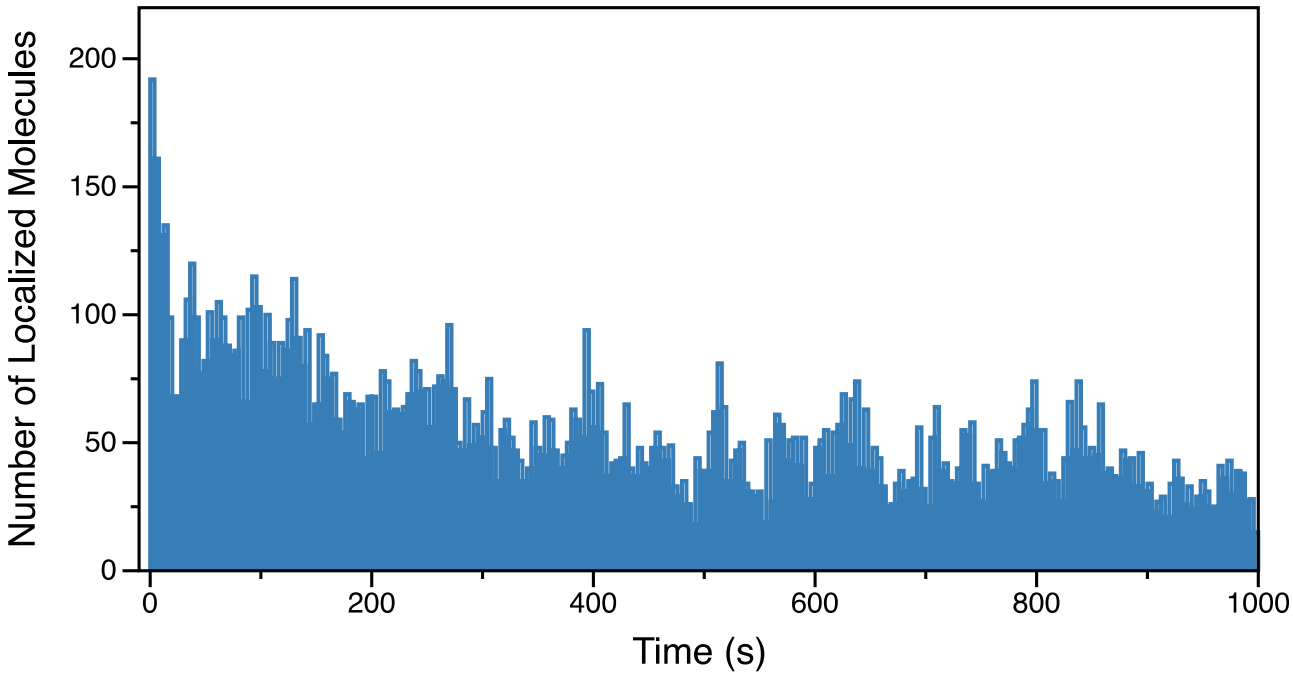

Figure S5. Changes in number of localized molecules after irradiation.

PXRD

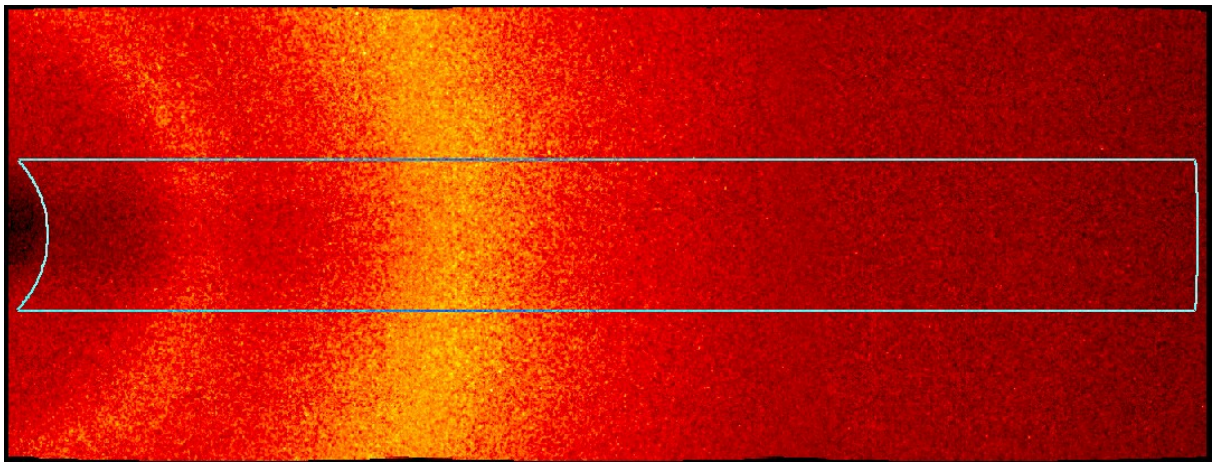

Figure S6. 2D-XRD data of **3** in the solid state.

Computational Data

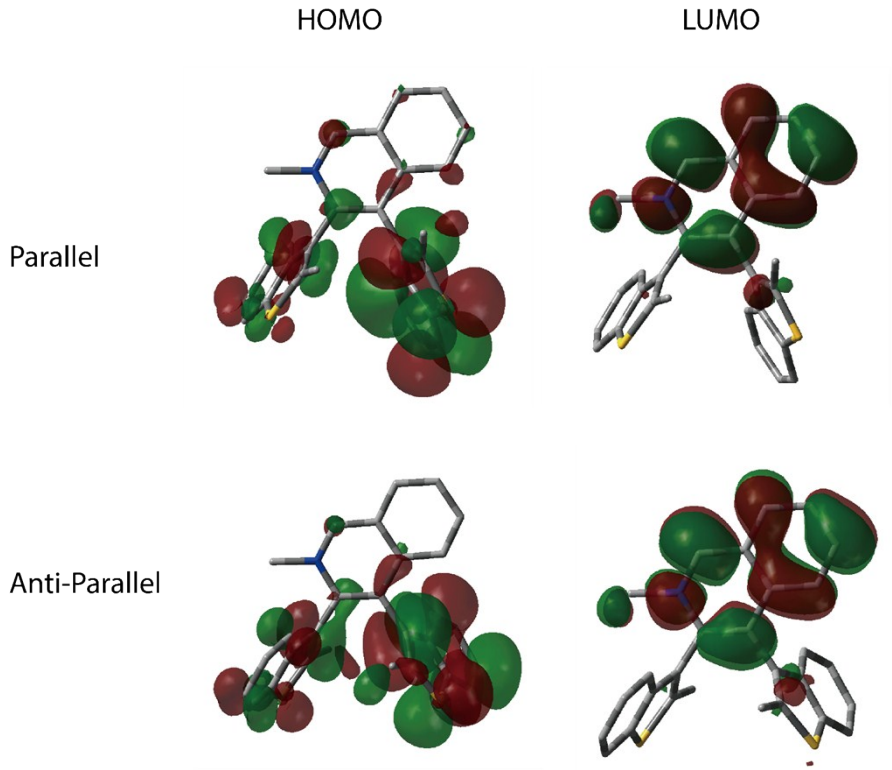

Figure S7. Frontier orbital diagrams of compound **3** in parallel and anti-parallel conformations.

Photoreaction Quantum Yield Determination

Chemical actinometry was employed for the photochemical quantum yield determination. Monochromated light generated by a fluorescence spectrometer was used to irradiate sample solutions. 313 nm was used for photocyclization reactions while 530 nm was used for photocycloreversion of **1c** and 486 nm for **2c**. The number of photons emitted per second by the irradiation source at specific wavelengths was calculated using ferrioxalate (313 nm) and Aberchrome 670 (486 nm and 530 nm) as standards following the literature procedure.[6-7]

$$N_p = \frac{v * n}{1000 * \varepsilon * \left(1 - 10^{-A'}\right) * \phi * l} * \frac{\Delta A}{\Delta t}$$

Where N_p is the number of photons emitted by the irradiation source, v solution volume (mL), n Avogadro's number, ε the absorption coefficient of ferrioxalate at 512 nm or Aberchrome 670 at 519 nm (L mol^{-1} cm^{-1}), A' the absorbance of the standards at the irradiation wavelength, ϕ the photoreaction quantum yield of the standards at certain irradiation wavelength, l the cell length (cm), ΔA the absorbance change of ferrioxalate at 512 nm or Aberchrome 670 at 519 nm, and Δt the time change.

The intensity of light at the irradiation wavelength was calculated:

313 nm: 5.11×10^{14} photons/s

486 nm: 1.47×10^{15} photons/s

530 nm: 9.1×10^{14} photons/s

Then photoreaction quantum yields of compound **1** and **2** can be calculated using the equation below:[8]

Photocyclization quantum yield (ϕ_{oc}):

$$A(t) - A(0) = \frac{1000 * \varepsilon * N_p * \left(1 - 10^{-A_{313}}\right) * \phi_{oc}}{n * v} * t$$

Photocycloreversion quantum yield (ϕ_{co}):

$$\log\left(10^{A(t)} - 1\right) - \log\left(10^{A(0)} - 1\right) = \frac{1000 * \varepsilon * l * N_p * \phi_{co}}{n * v} * t$$

Where $A(t)$ is the absorbance of **1** at 530 nm and **2** at 456 nm, ε the absorption coefficient of **1c** at 530 nm or **2c** at 486 nm, A_{313} the absorbance of **1o** and **2o** at 313 nm and assumed to be constant. ϕ_{oc} can be determined from the slope of the $A(t) - A(0)$ *vs.* t plots. ϕ_{co} can be determined from the slope of $\log\left(10^{A(t)} - 1\right) - \log\left(10^{A(0)} - 1\right)$ *vs.* t plots. Multiple experiments were carried out to obtain an average value.

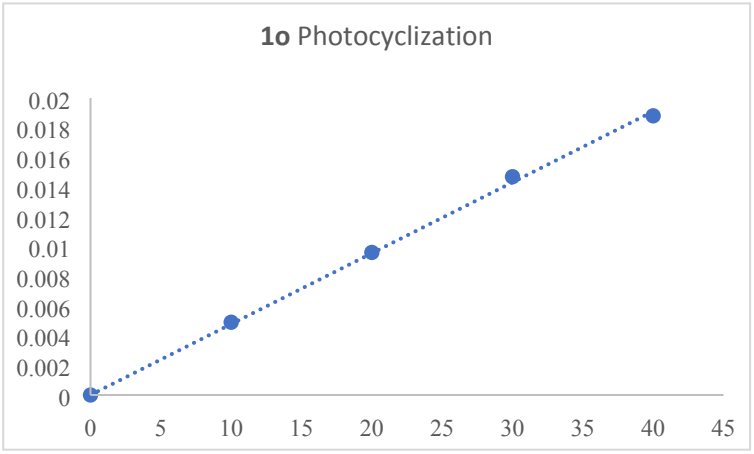

Figure S8. $A(t) - A(0)$ (@ 530 nm) *vs.* t plots of **1o** irradiated at 313 nm.

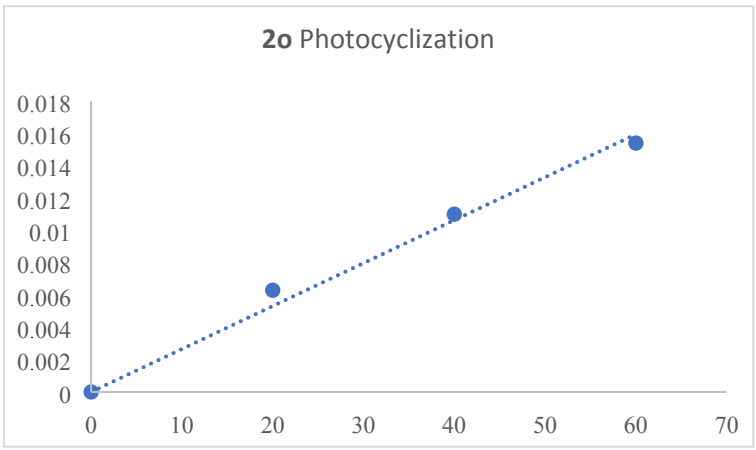

Figure S9. $A(t) - A(0)$ (@ 486 nm) *vs.* t plots of **2o** irradiated at 313 nm.

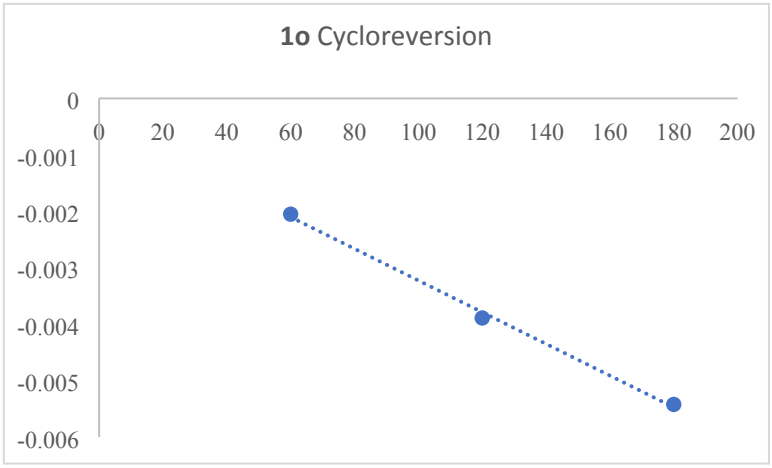

Figure S10. $\log\left(10^{A(t)} - 1\right) - \log\left(10^{A(0)} - 1\right)$ (@ 530 nm) *vs.* t plots of **1o** irradiated at 530 nm.

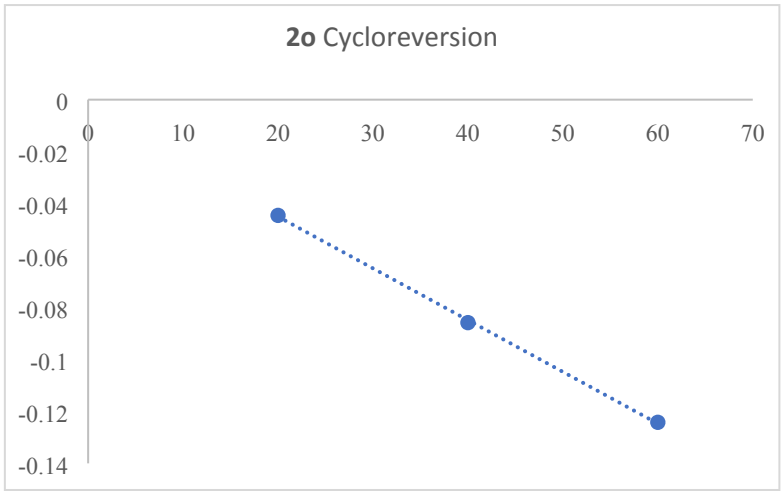

Figure S11. $\log\left(10^{A(t)} - 1\right) - \log\left(10^{A(0)} - 1\right)$ (@ 486 nm) *vs.* t plots of **2o** irradiated at 486 nm.

Reversibility

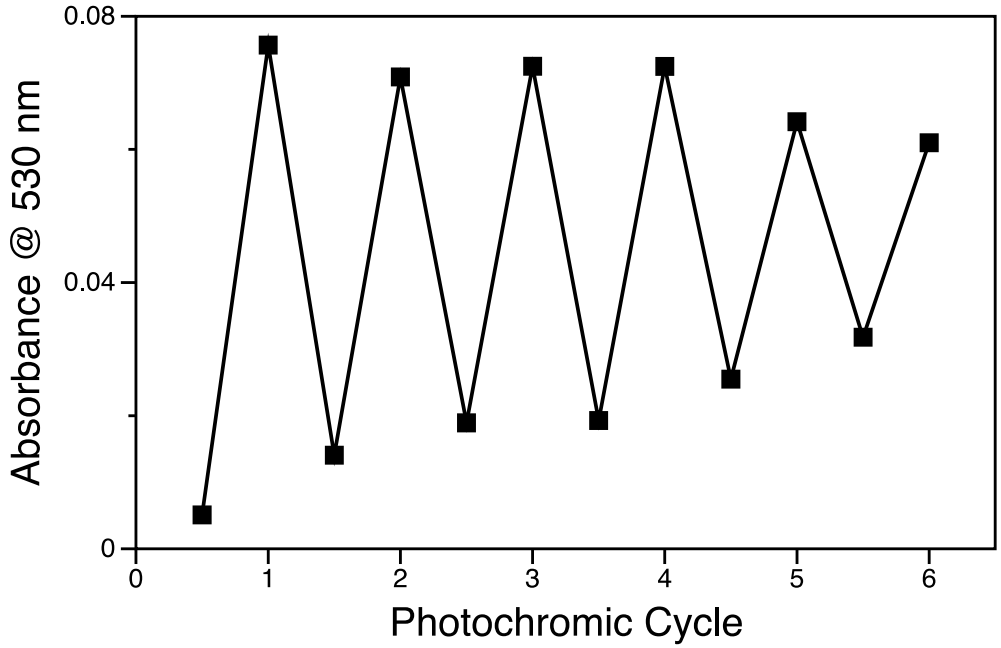

Figure S12. Absorbance changes at 530 nm of **1o** (~2.5 × 10^{-5} M) in DCM upon alternate excitation with 313 nm and 530 nm light over six cycles.

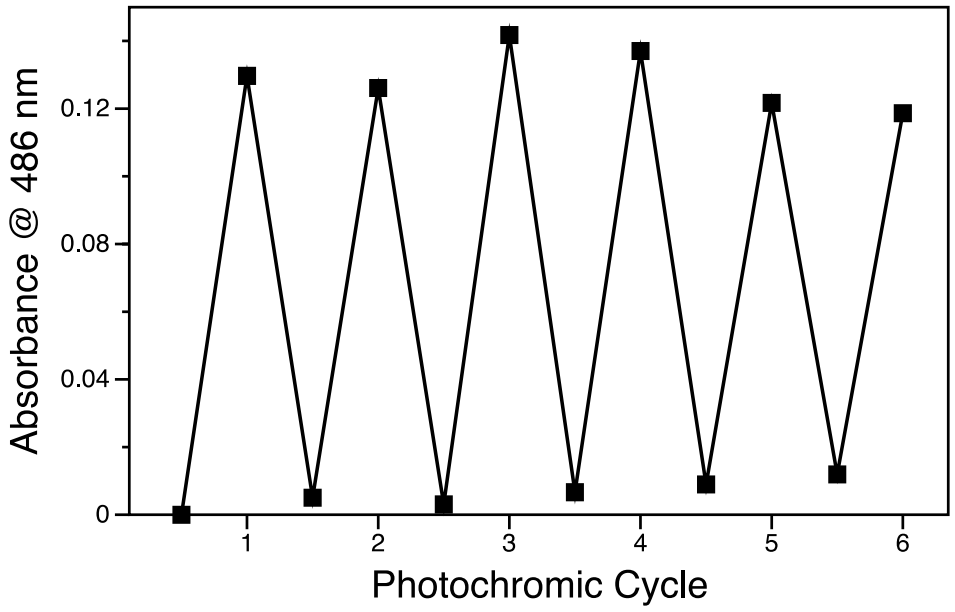

Figure S13. Absorbance changes at 486 nm of **2o** (~2.5 × 10^{-5} M) in DCM upon alternate excitation with 313 nm and 486 nm light over six cycles.

NMR Spectra

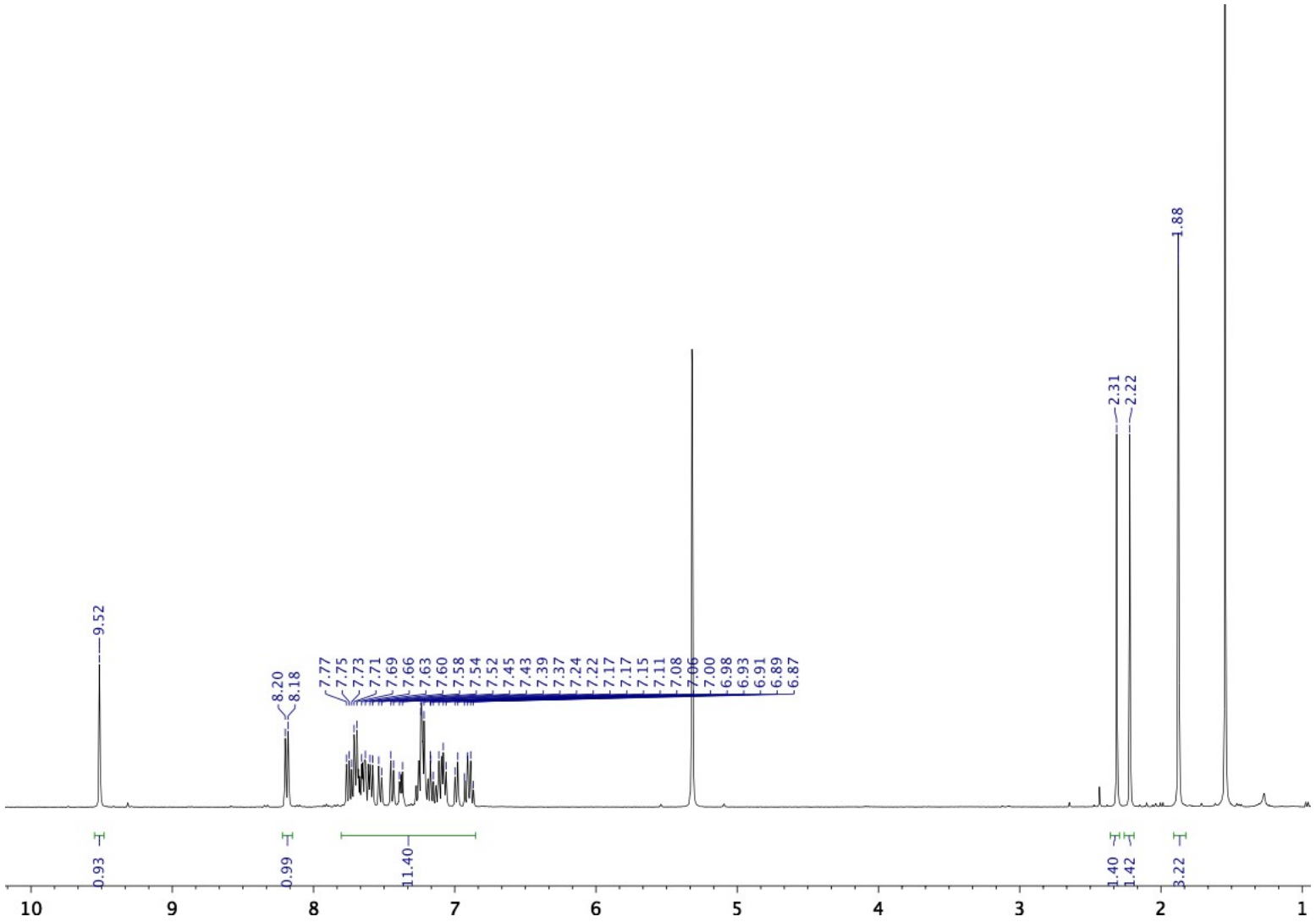

Figure S14. ^{1}H NMR spectrum of **1o** in CD_2Cl_2 at 25 ^{o}C

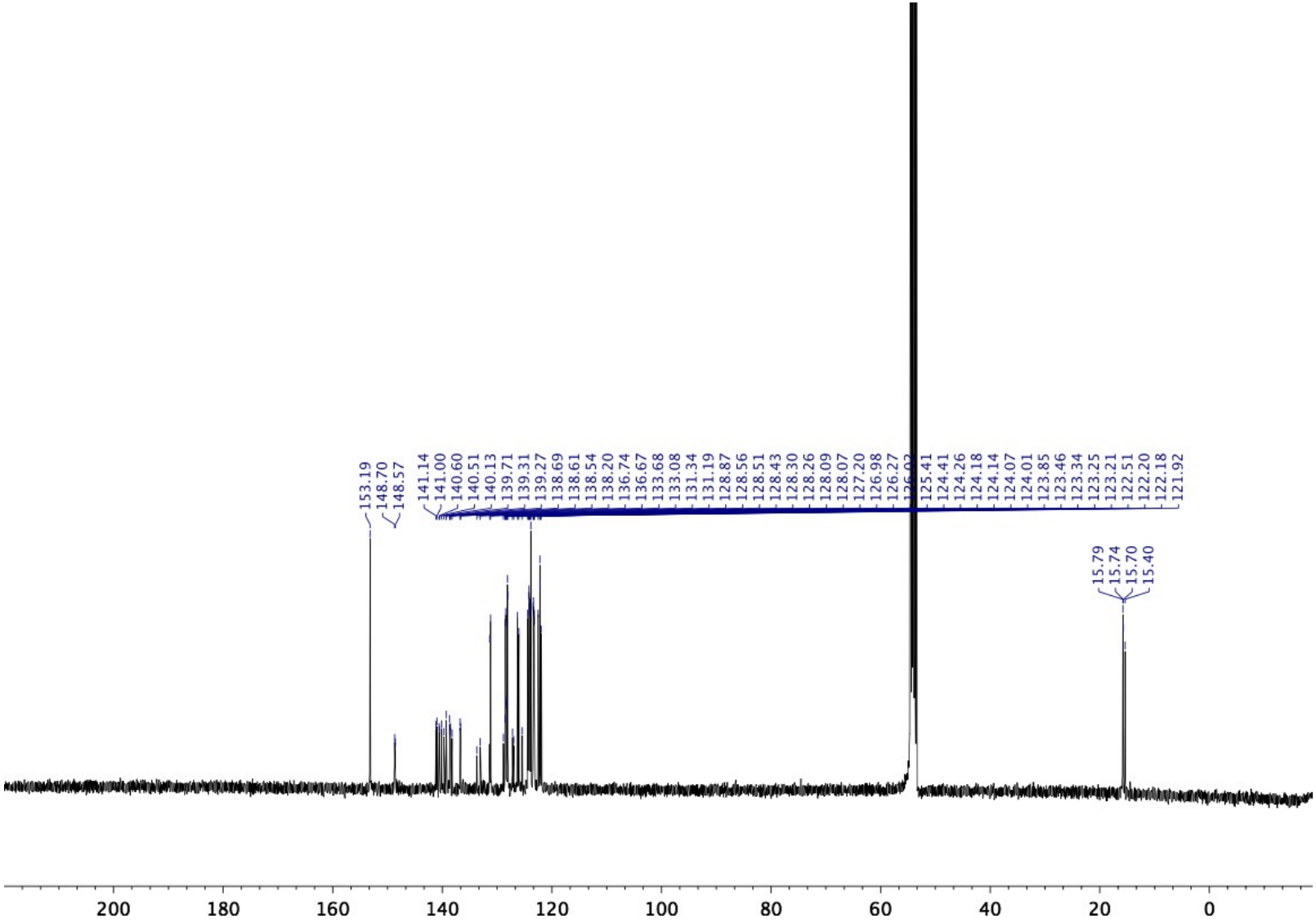

Figure S15. $^{13}C\{^{1}H\}$ NMR spectrum of **1o** in CD_2Cl_2 at 25 ^{o}C.

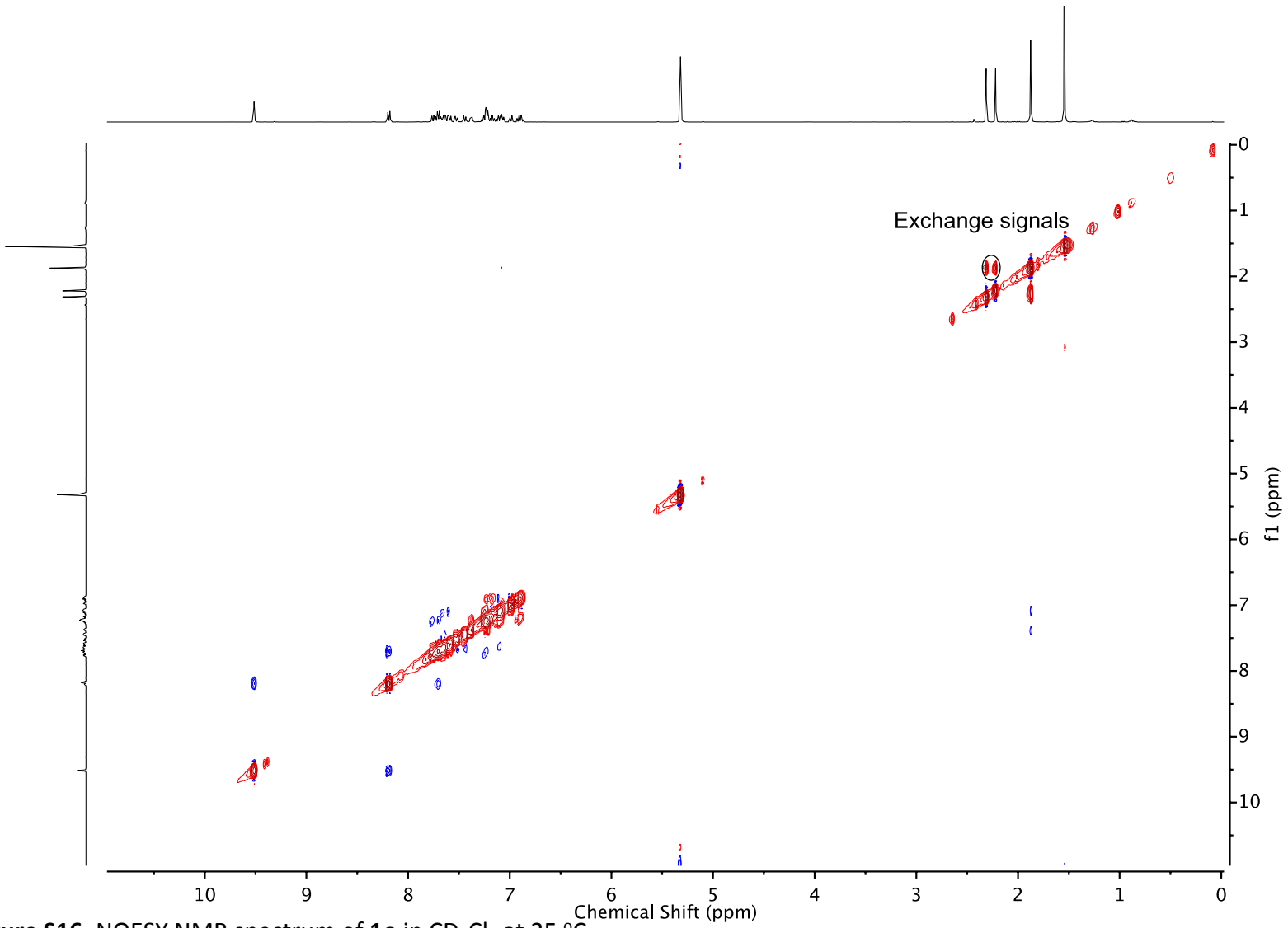

Figure S16. NOESY NMR spectrum of **1o** in CD_2Cl_2 at 25 °C.

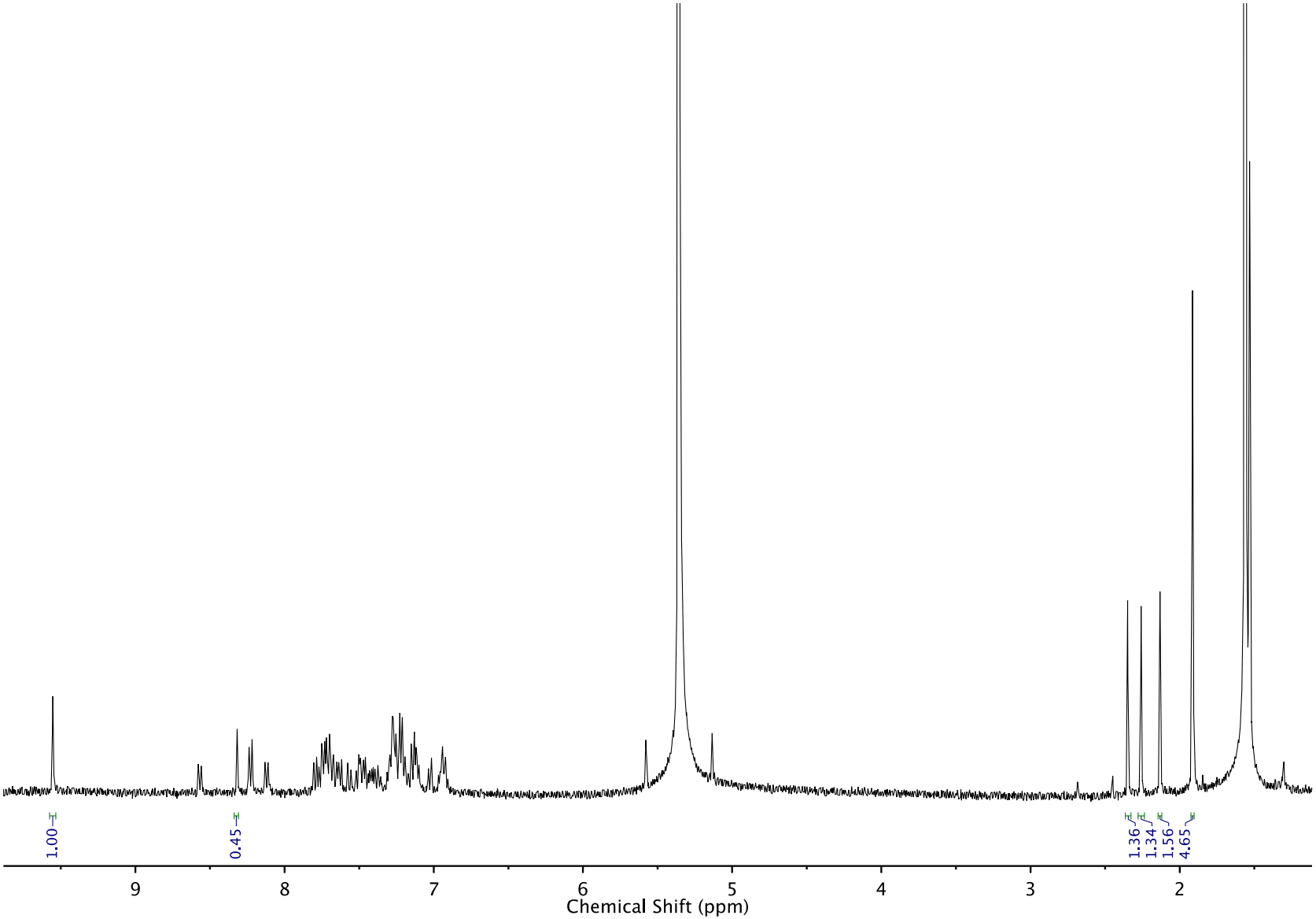

Figure S17. ^{1}H NMR spectrum of **1o** after irradiation in CD_2Cl_2 at 25 ^{o}C

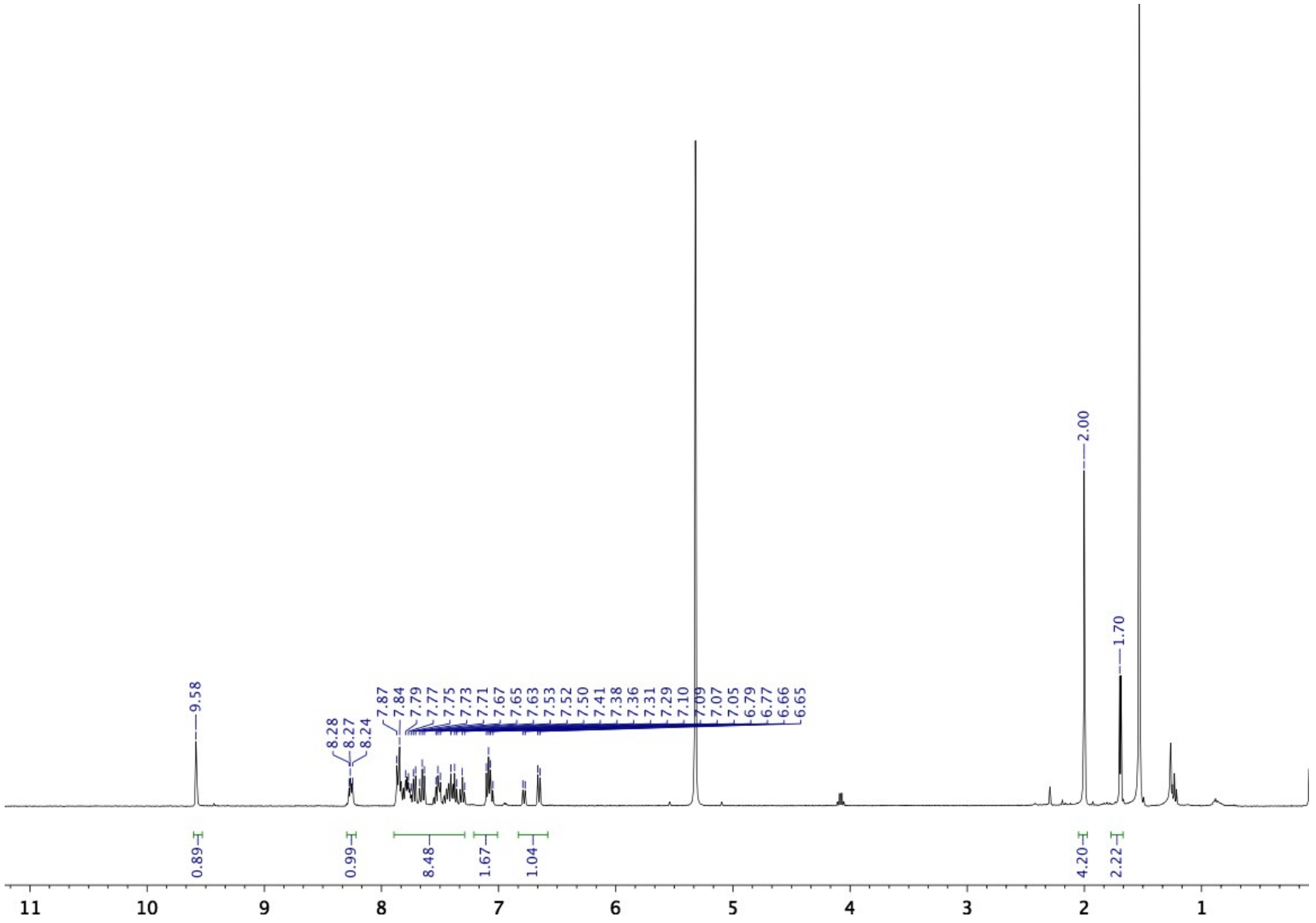

Figure S18. ^{1}H NMR spectrum of **2o** in CD_2Cl_2 at 25 ^{o}C.

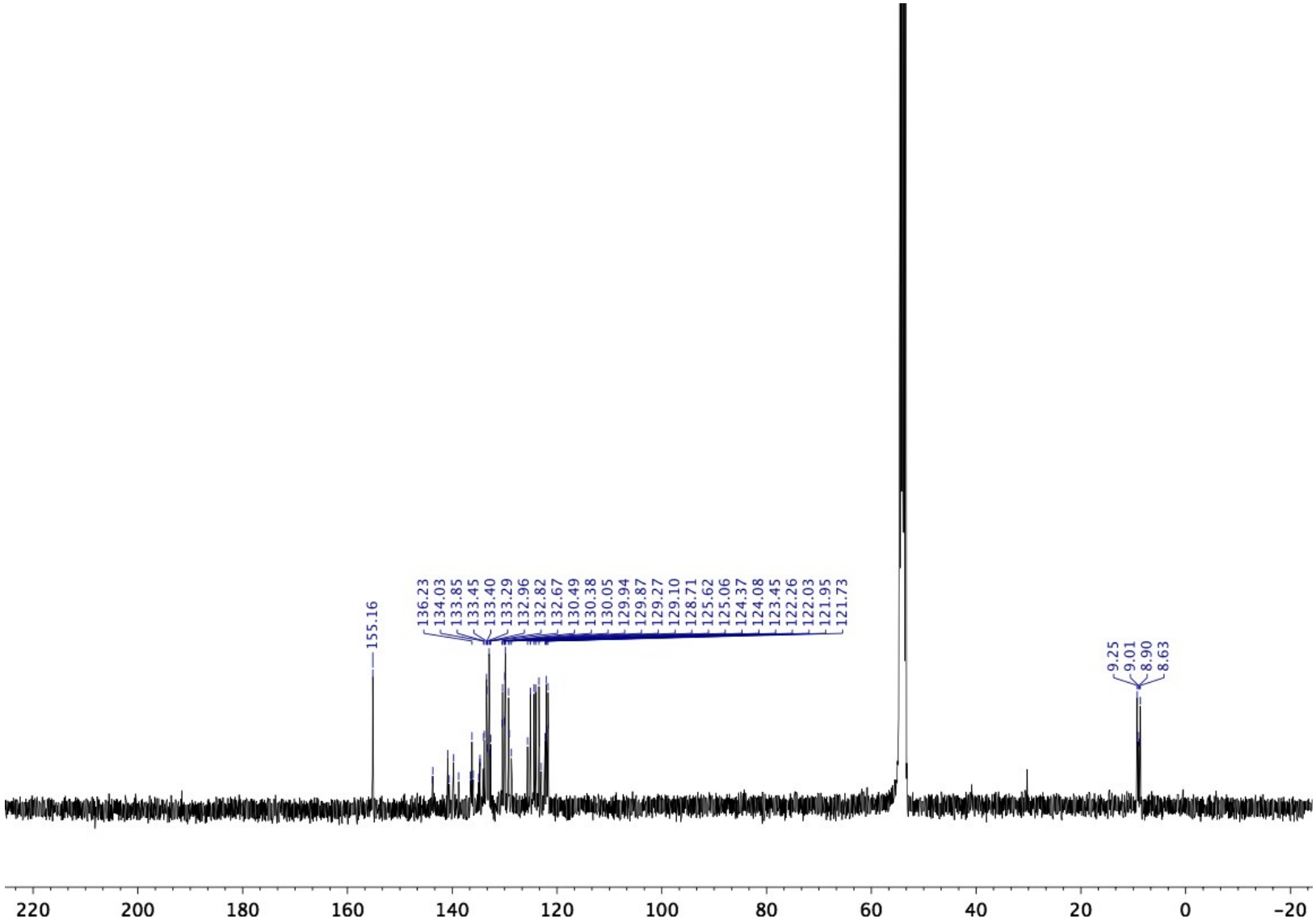

Figure S19. $^{13}C\{^{1}H\}$ NMR spectrum of **2o** in CD_2Cl_2 at 25 ^{o}C.

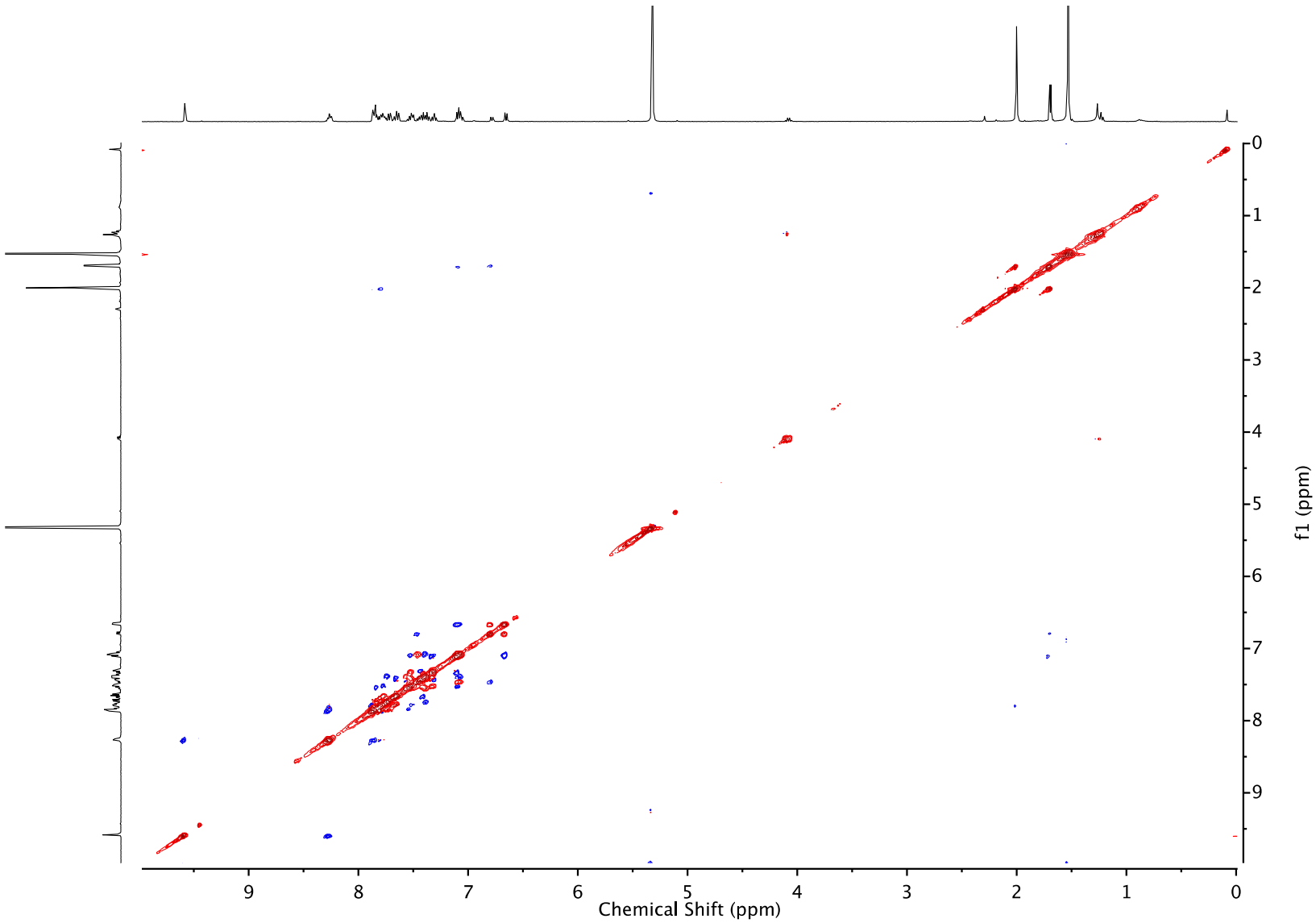

Figure S20. NOESY NMR spectrum of **2o** in CD_2Cl_2 at 25 °C.

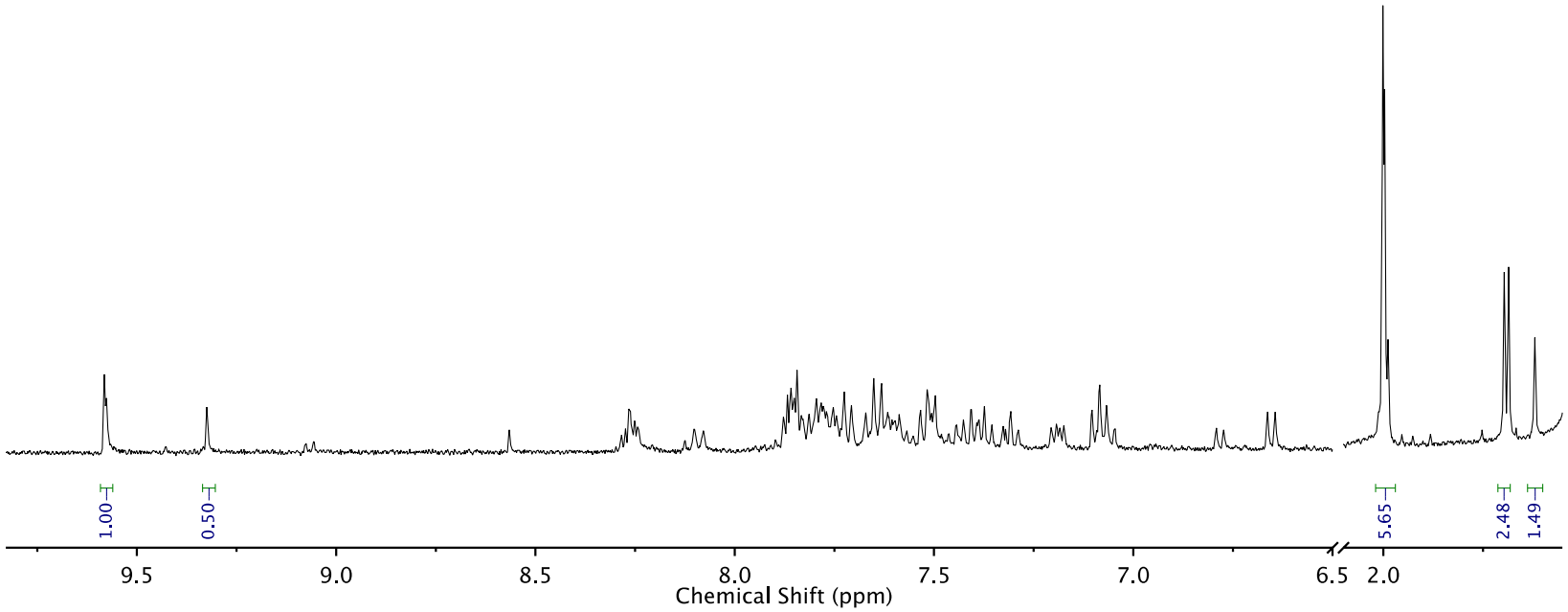

Figure S21. ^{1}H NMR spectrum of **2o** after irradiation in CD_2Cl_2 at 25 °C

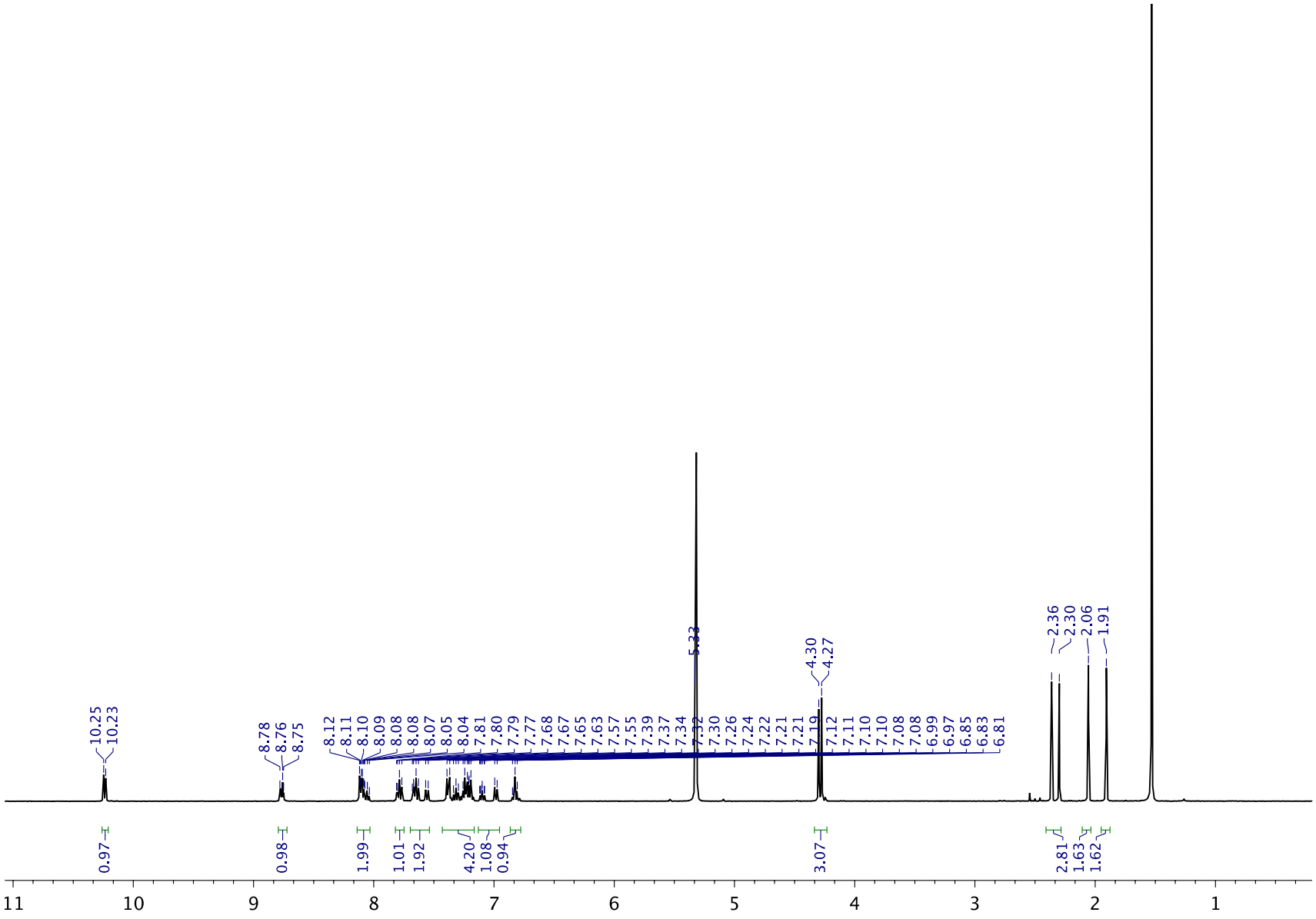

Figure S22. ^{1}H NMR spectrum of **3** in CD_2Cl_2 at 25 ^{o}C.

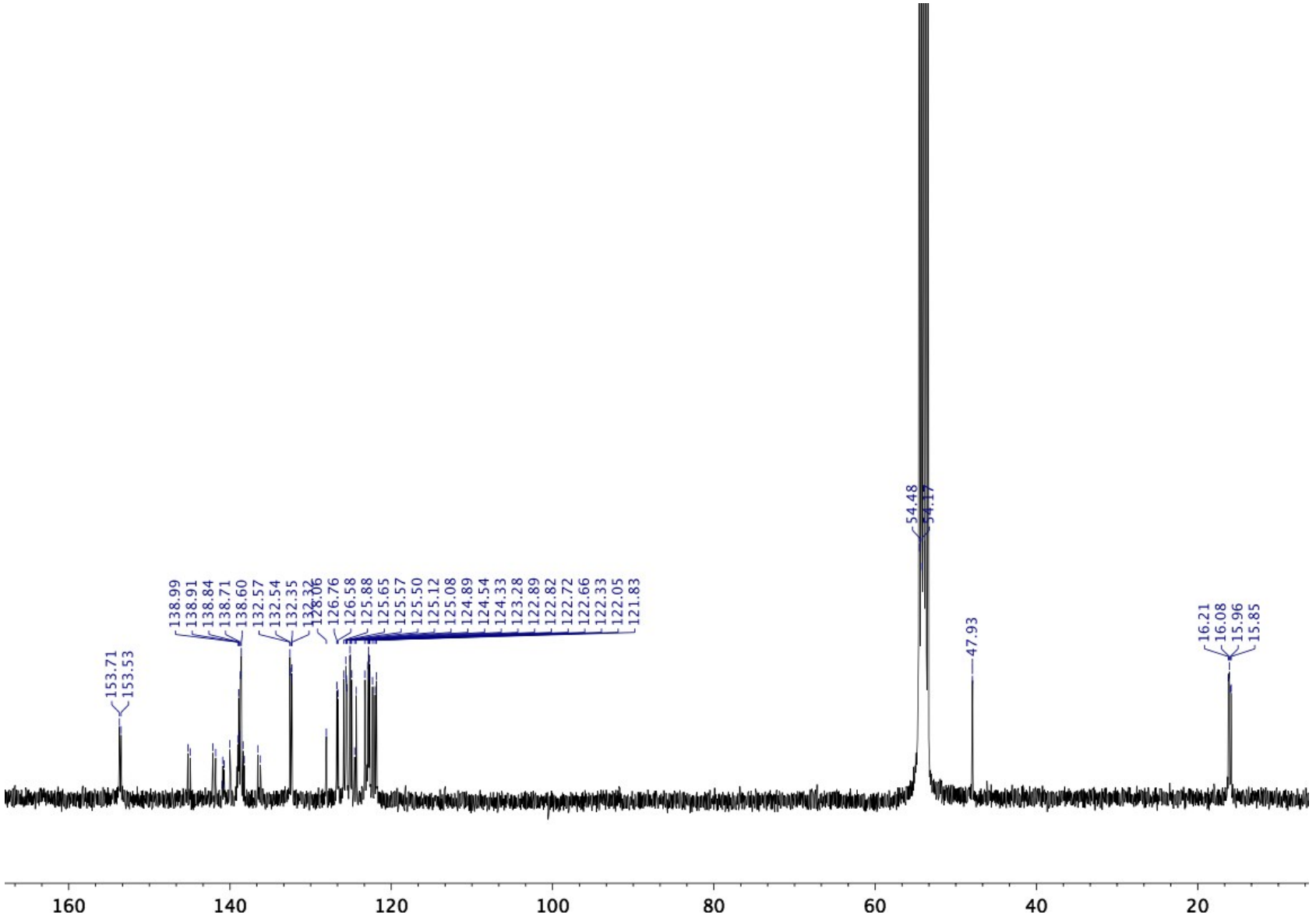

Figure S23. $^{13}C\{^{1}H\}$ NMR spectrum of **3** in CD_2Cl_2 at 25 °C.

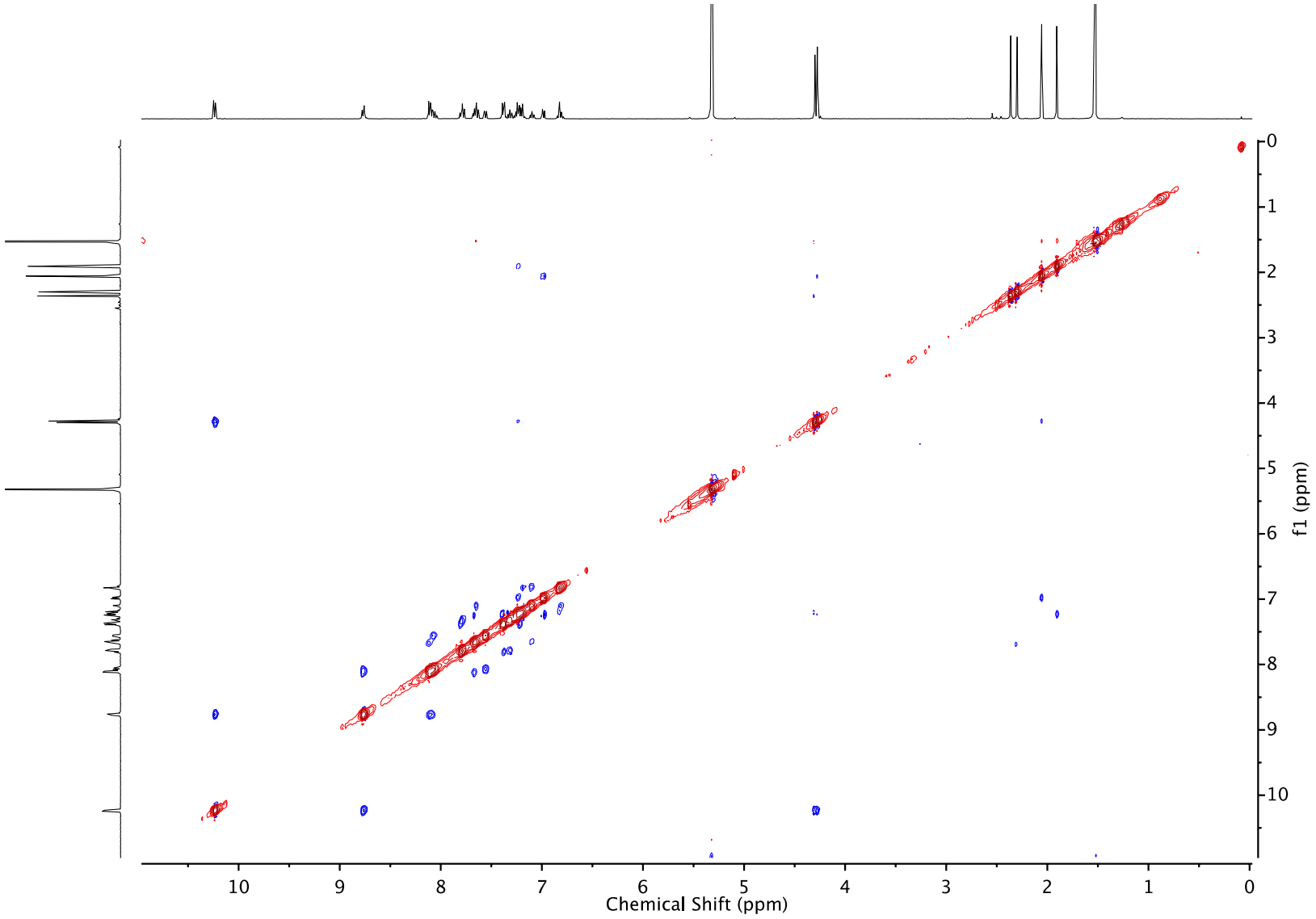
10
9
8
7
6
5
4
3
2
1
0
Chemical Shift (ppm)
0
1
2
3
4
5
6
7
8
9
10
f1 (ppm)

Figure S24. NOESY NMR spectrum of **3** in CD_2Cl_2 at 25 ^oC.

References

[1] S. Kawai, T. Nakashima, Y. Kutsunugi, H. Nakagawa, H. Nakano, T. Kawai, *J. Mater. Chem.* **2009**, *19*, 3606–3611.

[2] Q. Liu, L. Chen, H. C. Aguilar, K. C. Chou, *Nat. Commun.* **2018**, *9*, 3050.

[3] M. J. Frisch, G. W. Trucks, H. B. Schlegel, G. E. Scuseria, M. A. Robb, J. R. Cheeseman, G. Scalmani, V. Barone, G. A. Petersson, H. Nakatsuji, X. Li, M. Caricato, A. V. Marenich, J. Bloino, B. G. Janesko, R. Gomperts, B. Mennucci, H. P. Hratchian, J. V. Ortiz, A. F. Izmaylov, J. L. Sonnenberg, D. Williams-Young, F. Ding, F. Lipparini, F. Egidi, J. Goings, B. Peng, A. Petrone, T. Henderson, D. Ranasinghe, V. G. Zakrzewski, J. Gao, N. Rega, G. Zheng, W. Liang, M. Hada, M. Ehara, K. Toyota, R. Fukuda, J. Hasegawa, M. Ishida, T. Nakajima, Y. Honda, O. Kitao, H. Nakai, T. Vreven, K. Throssell, J. A. Montgomery, Jr., J. E. Peralta, F. Ogliaro, M. J. Bearpark, J. J. Heyd, E. N. Brothers, K. N. Kudin, V. N. Staroverov, T. A. Keith, R. Kobayashi, J. Normand, K. Raghavachari, A. P. Rendell, J. C. Burant, S. S. Iyengar, J. Tomasi, M. Cossi, J. M. Millam, M. Klene, C. Adamo, R. Cammi, J. W. Ochterski, R. L. Martin, K. Morokuma, O. Farkas, J. B. Foresman, and D. J. Fox, Gaussian, Inc., Wallingford CT, 2019.

[4] J. P. Perdew, M. Ernzerhof, K. Burke, *J. Chem. Phys.* **1996**, *105*, 9982-9985.

[5] C. Adamo, V. Barone, *J. Chem. Phys.* **1999**, *110*, 6158-6170.

[6] M. Montalti, A. Credi, L. Prodi, M. T. Gandolfi, *Handbook of Photochemistry*, CRC Press, **2006**.

[7] A. P. Glaze, H. G. Heller, J. Whittall, *J. Chem. Soc., Perkin Trans. 2* **1992**, 591–594.

[8] T. Sumi, Y. Takagi, A. Yagi, M. Morimoto, M. Irie, *Chem. Commun.* **2014**, *50*, 3928-3930.